Multiple Determinants Influence Complex Formation of the Hepatitis C Virus NS3 Protease Domain with Its NS4A Cofactor Peptide

Andrea Urbani,[‡,§] Gabriella Biasiol,[‡] Mirko Brunetti,[‡] Cinzia Volpari,[‡] Stefania Di Marco,[‡] Maurizio Sollazzo,[‡] Stefania Orrú,[‡] Fabrizio Dal Piaz,[||] Annarita Casbarra,[||] Piero Pucci,[||] Chiara Nardi,[‡] Paola Gallinari,[‡] Raffaele De Francesco,[‡] and Christian Steinkühler*[,‡]

Istituto di Ricerche di Biologia Molecolare, "P. Angeletti" Via Pontina Km 30,600, Pomezia, 00040 Rome, Italy, and Centro Internazionale di Servizi di Spettrometria di Massa, CNR-Università di Napoli Federico II, via Pansini 5, 80131 Napoli, Italy

Received November 23, 1998; Revised Manuscript Received January 25, 1999

ABSTRACT: The interaction of the hepatitis C virus (HCV) NS3 protease domain with its NS4A cofactor peptide (Pep4AK) was investigated at equilibrium and at pre-steady state under different physicochemical conditions. Equilibrium dissociation constants of the NS3−Pep4AK complex varied by several orders of magnitude depending on buffer additives. Glycerol, NaCl, detergents, and peptide substrates were found to stabilize this interaction. The extent of glycerol-induced stabilization varied in an HCV strain-dependent way with at least one determinant mapping to an NS3−NS4A interaction site. Conformational transitions affecting at least the first 18 amino acids of NS3 were the main energy barriers for both the association and the dissociation reactions of the complex. However, deletion of this N-terminal portion of the protease molecule only slightly influenced equilibrium dissociation constants determined under different physicochemical conditions. Limited proteolysis experiments coupled with mass spectrometric identification of cleavage fragments suggested a high degree of conformational flexibility affecting at least the first 21 residues of NS3. The accessibility of this region of the protease to limited chymotryptic digestion did not significantly change in any condition tested, whereas a significant reduction of chymotryptic cleavages within the NS3 core was detected under conditions of high NS3−Pep4AK complex affinity. We conclude the following: (1) The N-terminus of the NS3 protease that, according to the X-ray crystal structure, makes extensive contacts with the cofactor peptide is highly flexible in solution and contributes only marginally to the thermodynamic stability of the complex. (2) Affinity enhancement is accomplished by several factors through a general stabilization of the fold of the NS3 molecule.

Hepatitis C is a major health problem affecting about 0.5−1.5% of the world's population. The disease is caused by a viral infectious agent, the hepatitis C virus (HCV[1]), whose major route of transmission is parenteral (*1*−*3*). The virus was identified by molecular cloning in 1989 (*1*), and its genome, a 9.5-kilobase single-stranded positive sense RNA molecule, contains a single open reading frame encoding a polyprotein of 3010−3033 residues. Upon its synthesis in cells, this polyprotein is processed into the mature polypeptides through the combined action of both cellular signal peptidases and two virally encoded proteolytic enzymes (reviewed in ref *4*). The serine protease domain contained in the viral NS3 protein appears to play a prominent role in the processing of the HCV polyprotein. It is responsible for 4 out of the 5 cleavage events that have to take place in order to generate the mature nonstructural proteins believed to form the replication machinery of the virus. The NS3-dependent processing occurs at the intramolecular NS3/NS4A site and at the intermolecular NS4A/NS4B, NS4B/NS5A, and NS5A/NS5B cleavage sites of the HCV polyprotein. Besides containing a serine protease domain of about 20 kDa at its N-terminus, the NS3 protein harbors an RNA helicase in its ∼400 C-terminal residues (*5*). Deletion experiments have shown that helicase and protease domains can work independently of each other, with the separate polypeptide chains expressing the respective activities (*5*−*12*). This has recently permitted the crystallization of the NS3 protease and helicase domains (*13*−*16*).

Although the NS3 protease has proteolytic activity of its own, in vivo complex formation with the viral NS4A protein is essential for efficient processing of the NS3/NS4A and NS4B/NS5A sites and improves cleavage at the NS4A/NS4B and NS5A/NS5B junctions (*6*, *17*−*19*). NS4A is a protein of 54 residues. According to hydropathy plots and secondary structure prediction algorithms it can be subdivided into three portions: residues 1−34 are highly hydrophobic with the first 20 residues predicted to have a high propensity of forming an α-helix, whereas residues 21−34 are assumed to preferentially form β-strands. The remaining 20 C-terminal residues of NS4A are hydrophilic with a preference for

* To whom correspondence should be addressed: IRBM, Via Pontina Km 30,600-00040 Pomezia, Italy. Phone: ++39 06 91093232. Fax: ++39 06 91093225. E-mail: Steinkuhler@IRBM.it.

[‡] Istituto di Ricerche di Biologia Molecolare.

[§] Present address: European Molecular Biology Laboratory (EMBL), Meyerhofstrasse 1, Postfach 102209, D-69012 Heidelberg, Germany.

[||] CNR-Università di Napoli Federico II.

[1] Abbreviations: CHAPS, 3-(3-cholamidopropyl) dimethylammonio-1-propanesulfonate; DTT, dithiothreitol; HCV, hepatitis C virus; NS, nonstructural; LDAO, lauryldimethylamine oxide; TFA, trifluoracetic acid.

10.1021/bi982773u CCC: $18.00
Published on Web 04/02/1999

adopting a helical conformation. Deletion mutagenesis experiments have shown that residues 21−34, corresponding to the extended, hydrophobic region of NS4A, are sufficient for eliciting full activation of the NS3 protease (*12*, *17*, *20*−*22*). In vitro, NS3 can be activated by the addition of a peptide harboring this central region of the NS4A cofactor (*12*, *20*−*22*). This peptide has also been crystallized in a complex with the NS3 protease domain (*13*, *15*). The structural data show that the bound cofactor is embedded into the core of the NS3 protease domain with a total of 2400 Å^2 of surface area buried by the interaction between the two molecules. The N-terminus of NS3 that is involved in this interaction has a peculiar $\beta-\alpha-\beta$ fold with a β-strand contributed by the cofactor intercalating into this structure. In vivo the native NS3−NS4A complex is thought to be associated with membranes (*19*). Membrane anchoring could be provided by the extreme N-terminus of NS4A that was proposed to form a trans-membrane helix (*15*). Deletion mutagenesis experiments demonstrated that in vivo either "loose" or "tight" complexes can be formed, depending on the integrity of the N-terminus of NS4A (*18*, *23*). In addition, the α-helical portion of the $\beta-\alpha-\beta$ fold at the N-terminus of NS3 was proposed to participate in membrane anchoring, since hydrophobic residues on this helix (Ile14, Leu17, Ile18, and Leu21) face outward from the complex to create a hydrophobic area (*15*). In the structure without NS4A, the N-terminus of NS3 interacts with neighboring molecules binding to hydrophobic surface patches (*14*). These interactions are likely to be peculiar features of the crystallized enzyme, and in solution, the N-terminal region of NS3 is probably disordered in the absence of NS4A, thus providing an explanation for the enhanced metabolic stability of the NS3−NS4A complex with respect to the uncomplexed enzyme (*15*). Enhancement of protease activity upon complexation appears to result from the correct positioning of His57, Asp81, and Ser139, the residues that form the catalytic triad of the enzyme. In the absence of NS4A, Asp81 is tilted away from His57, interacting with the guanidinium moiety of a nearby arginine residue (Arg155) (*14*, *24*). Also His57 and the catalytic Ser139 are too far away to engage in hydrogen bond interactions in the free enzyme. This conformation is clearly unfavorable for proton shuttle during catalysis, whereas in the complexed enzyme, the catalytic triad assumes a structural organization that is also observed in other serine proteases.

We have previously shown that complex formation between the truncated NS3 protease and an NS4A peptide goes along with changes in the protein near-UV CD spectrum and in its tryptophan fluorescence spectrum (*25*). These spectroscopic findings were interpreted in terms of changes in the environment of Trp85, which is engaged in the interaction with Val23 of the cofactor peptide, and have allowed the calculation of the equilibrium dissociation constants in the low micromolar range and a complex half-life of 3.5 min (*25*). These values are indicative of a relatively loose complex and are poorly compatible with the extensive interaction that is observed in the crystal structure. In the present study we have therefore investigated complex formation in solution using pre-steady-state and equilibrium measurements of complex affinity to identify factors that influence the binding reaction. We have also attempted to correlate some kinetic and thermodynamic information with structural data using site-directed mutagenesis, fluorescence spectroscopy, and limited proteolysis/mass spectrometry as analytical tools. We show that complex affinities may differ by almost 3 orders of magnitude depending on the physicochemical conditions under which they are determined. Complex stabilities under a given condition may further vary significantly for NS3 proteases from different HCV isolates, with at least one of the affinity determinants mapping to an NS3−NS4A interaction site. In addition, we also present evidence for complex stabilization by substrate peptides to the active site of the enzyme, suggesting a cross-talk between the substrate binding site and the cofactor binding site.

MATERIALS AND METHODS

Enzyme Preparations and Site-Directed Mutagenesis. *Escherichia coli* BL21(DE3) cells were transformed with plasmids containing the cDNA coding for the serine protease domains of the HCV BK or J-strains NS3 protein (amino acids 1027−1206, followed by a solubilizing ASKKKK tag) under the control of the bacteriophage T7 gene 10 promoter in a pT7-7 vector. The V36L, Q86P, and V36L + Q86P mutations were introduced into the lysine-tagged Bk-strain protease by PCR using appropriate primers. Proteins encompassing residues 1027−1213 and 1045−1213 (NS3−J−ΔN) from the HCV J-strain were also obtained by PCR. All constructs were fully sequenced on both strands to exclude introduction of additional mutations by PCR. Enzymes were purified as previously described (*26*) and found to be homogeneous as judged from silver-stained SDS−PAGE and >95% pure as judged from reversed-phase HPLC performed using a 4.6 × 250 mm Vydac C4 column. Enzyme preparations were routinely checked by mass spectrometry done on HPLC-purified samples using a Perkin-Elmer API 100 instrument and by N-terminal sequence analysis carried out using Edman degradation on an Applied Biosystems model 470A gas-phase sequencer. Enzyme stocks were quantified by amino acid analysis, shock-frozen in liquid nitrogen, and kept in aliquots at −80 °C until use.

Peptides and HPLC Assays. Synthetic peptides were obtained from AnaSpec, Inc. (San Jose) and Peptides International, Inc. (Louisville). The concentration of stock solutions of peptides, prepared in DMSO or in buffered aqueous solutions and kept at −80 °C until use, was determined by quantitative amino acid analysis performed on HCl-hydrolyzed samples.

If not specified differently, cleavage assays were performed in 57 μL of 50 mM Tris, pH 7.5, 10 mM DTT to which differing amounts of glycerol, detergents, and NaCl were added. Reactions were started by the addition of 3 μL of substrate peptides. Six duplicate data points at substrate concentrations between $K_m/4$ and $4K_m$ were used to calculate kinetic parameters. As protease cofactor we used a peptide spanning the central hydrophobic core (residues 21−34) of the NS4A protein, containing a solubilizing lys tag at its N-terminus (Pep4AK (KKKGSVVIVGRIILSGR(NH_2)). Incubation times and enzyme concentrations were chosen in order to obtain <8% substrate conversion. Reactions were stopped by the addition of 40 μL of 1% TFA. Cleavage of peptide substrates was determined by HPLC as previously described (*27*). Cleavage products were quantified by the integration of chromatograms with respect to appropriate

standards. Kinetic parameters were calculated from a nonlinear least-squares fit of initial rates as a function of substrate concentration with the help of a Kaleidagraph software, assuming Michaelis−Menten kinetics.

Kinetic determination of K_d values was performed at a fixed substrate concentration. K_d values were calculated by a nonlinear least-squares fitting of eq 1 to the data points

$$V = V_0 + (V_{max}[\text{Pep4AK}])/(K_{d\ app} + [\text{Pep4AK}]) \quad (1)$$

with V_0 being the velocity in the absence of the cofactor, V the initial velocity of enzymatic catalysis at a given Pep4AK concentration, V_{max} the velocity at Pep4AK saturation, and $K_{d\ app}$ the apparent dissociation constant of the NS3−Pep4AK complex.

Fluorescence Measurements. Fluorescence emission spectra were recorded on a Perkin-Elmer LS50B instrument with a cuvette holder thermostated at 23 °C. Excitation was at 295 nm and emission was recorded between 300 and 400 nm at a scan speed of 60 nm/min. Emission and excitation slits were opened to 5 nm. Spectra were routinely corrected for the background signal of buffer and for dilution effects. Equilibrium dissociation constants were calculated from fluorescence data by fitting expression 2 to the data

$$\Delta F = F_0 + ((\Delta F_{max}\text{Pep4AK})/(K_d + \text{Pep4AK})) \quad (2)$$

where F_0 is the initial fluorescence in the absence of added Pep4AK, ΔF is the fluorescence increase at 333 nm induced by a given concentration of Pep4AK, and ΔF_{max} is the fluorescence increase observed at enzyme saturation. pH dependence experiments were done using a three-component buffer containing 25 mM Tris, 12.3 mM acetate, 12.3 mM Mes, 15% glycerol, 1% CHAPS, and 150 mM NaCl. pH-dependent variations of ionic strength were corrected by the addition of NaCl.

Pre-Steady-State Measurements. Association rate constants were determined on an SX-MV18 Applied Photophysics stopped-flow instrument equipped with a fluorescence detector and interfaced with a Risc computer. The samples and the flow cell were thermostated at 23 °C. Protein fluorescence was excited at 280 nm, and a 305 nm cutoff filter was used to suppress the excitation wavelength. Time-dependent fluorescence changes upon addition of Pep4AK to the NS3 protease were recorded under pseudo-first-order conditions for at least $5 \times t/2$ and could be best fitted to a single-exponential equation. k_{obs} values derived from this fitting procedure were determined at different Pep4AK concentrations and used to calculate association rate constants according to eq 3.

$$k_{obs} = k_{off} + k_{on}[\text{Pep4AK}] \quad (3)$$

Equilibrium dissociation constants (K_d values) were calculated from the dependence of the amplitude of the fluorescence change on the concentration of Pep4AK according to eq 2. Dissociation rate constants (k_{off} values) were subsequently calculated from the expression $k_{off} = k_{on}K_d$. In selected cases dissociation rate constants were also directly measured by monitoring the decrease in fluorescence intensity upon rapid dilution of preformed NS3−Pep4AK complexes at concentrations below their K_d values. A good agreement (less than 15% deviation) was observed between values obtained with either method.

Limited Proteolysis Experiments. Enzymatic digestions were performed at 25 °C in the appropriate buffer system using trypsin, chymotrypsin, subtilysin, or Lys C in a 1:100 or 1:500 (w/w) enzyme-to-substrate ratio. The extent of the reaction was monitored on a time-course basis by sampling the incubation mixture at different time intervals. Proteolytic fragments were fractionated by reverse-phase HPLC on a Vydac C18 column, and the individual fractions were manually collected and analyzed using a Bio-Q triple quadrupole mass spectrometer (Micromass, Manchester, UK) equipped with an electrospray ion source. Samples were injected into the ion source (kept at 80 °C) via a loop injection at a flow rate of 10 μL/min. Data were acquired and elaborated using the MASSLYNX program, purchased from Micromass. Mass calibration was performed by means of multiply charged ions from a separate injection of horse heart myoglobin (Sigma; average molecular mass of 16951.5 Da).

RESULTS

Glycerol Dependence of the Affinity of the NS3−Pep4AK Complex. There are several methods by which the affinity of the NS3 protease for the NS4A cofactor peptide (Pep4AK) can be determined (*25*). Conveniently, titration of the enhancement of proteolytic activity as a function of added Pep4AK at a fixed substrate concentration can be used as a technique. In this case, the affinity of Pep4AK for the enzyme−substrate complex is measured, provided that the experiment is performed at a saturating substrate concentration ($[S] \gg K_m$). At lower substrate concentrations, apparent dissociation constants, reflecting the affinities for both the enzyme−substrate complex and the free enzyme, will be obtained. The affinity of Pep4AK for the free enzyme can also be directly monitored, taking advantage of the changes in the tryptophan fluorescence spectra observed upon complex formation (*25*). For the NS3 protease domain of the HCV Bk-strain it has been previously shown that in the presence of 50% glycerol the substrate peptide Ac-DEMEE-CASHLPYK, substrate **S1**, derived from the NS4AB junction of the HCV polyprotein has little effect on the dissociation constant of the enzyme−cofactor complex (*25*). Titration experiments of the Pep4AK dependence of proteolytic activity have shown that glycerol is an important requirement for complex formation between the NS3 protease domain from the HCV Bk-strain and its NS4A cofactor. Unexpectedly, we found that this glycerol dependence was much less pronounced for the NS3 protease domain of the HCV J-strain (Table 1). Sequence comparison has shown that, while the sequence of the central domain of NS4A is identical in both strains, the two NS3 protease domains differ for 8, mostly conservative, point mutations. Three sequence variations between NS3−BK and NS3−J, namely Glu30-Asp, Val36-Leu, and Gln86-Pro, are located in the N-terminal region of the NS3 molecule that is involved in complex formation with the cofactor. Gln86 is located adjacent to Trp85. Alterations in the physicochemical environment of this latter residue have been suggested to occur upon complex formation with Pep4AK, based on changes in fluorescence and near-UV circular dichroism spectra (*25*). These changes are thought to result from binding of Val23 of the NS4A cofactor into a

Table 1: Glycerol Dependence of the Apparent Equilibrium Dissociation Constant K_d of the NS3−Pep4AK Complex[a]

enzyme	K_d (μM) at glycerol concentration			
	0%	15%	30%	50%
Bk	>100	>100	58	5.3
J	60	25	5.5	1.3
Bk Q86P	>100	98	32	3.2
Bk V36L	>100	54	15	4.6
Bk Q86P + V36L	>100	24	8	2.3

[a] Dissociation constants were determined kinetically as described under Materials and Methods. Assays were performed in 50 mM Tris, pH 7.5, 1% CHAPS, 10 mM DTT, and varying amounts of glycerol in the presence of 20 μM substrate DEMEECASHLPYK.

hydrophobic pocket of NS3 flanked, among other residues, also by Trp85 and Val36. Both the Gln86-Pro and the Val36-Leu mutations could therefore potentially alter the shape of this pocket and hence influence the stability of the enzyme−cofactor complex. This was experimentally verified by introducing the Gln86-Pro and Val36-Leu mutations in the context of the Bk sequence, both as single and as double mutants. The apparent dissociation constants of the mutated enzymes were then determined at different glycerol concentrations in the presence of a fixed substrate concentration. As shown in Table 1, the Gln86-Pro mutation lead to no significant alterations in the glycerol dependence of cofactor binding. In contrast, substitution of Val36 for leucine leads to an improved affinity of the mutant enzyme for Pep4AK at glycerol concentrations <50%, whereas the double mutant Val36-Leu + Gln86-Pro was indistinguishable within experimental accuracy from the J-strain enzyme at glycerol concentrations between 15% and 50% (Table 1), but showed a significantly lower affinity in the absence of glycerol. These data demonstrate that Leu36 contributes considerably to the stabilization of the NS3−Pep4AK complex.

So far, all Pep4AK affinity data have been generated in the presence of the substrate peptide **S1** by monitoring the enhancement of protease activity produced upon cofactor binding. We next decided to investigate complex formation between the free enzyme and its cofactor by monitoring the fluorescence changes that accompany the binding event (Figure 1A−C). These changes were monitored both under pre-steady-state conditions (Figure 1A) and upon attainment of thermodynamic equilibrium (Figure 1C) using a stopped-flow instrument. Table 2 reports the steady-state equilibrium dissociation constants (K_d), the association rate constants (k_{on}), and the dissociation rate constants (k_{off}) obtained with the J, Bk, BkV36L, and BkQ86P + V36L enzymes at a fixed glycerol concentration of 30% and in the presence of 1% CHAPS. Under these conditions, the affinity of the J-strain enzyme for the cofactor is about 65-fold higher than that of the Bk enzyme. The nature of this difference was explored by pre-steady-state measurements. Plots of k_{obs} versus cofactor concentration were linear for all enzymes (Figure 1B) and were used to calculate association rate constants according to eq 3. The pre-steady-state analysis revealed that the difference in the equilibrium dissociation constants between the two enzymes results from both a 3.8-fold higher association rate constant and a 18.5-fold lower dissociation rate constant (Table 2). The V36L mutant shows a 6.9-fold increased on-rate with respect to the wild type enzyme but little effect on the off-rate, confirming that this residue significantly contributes to complex stabilization, but is not

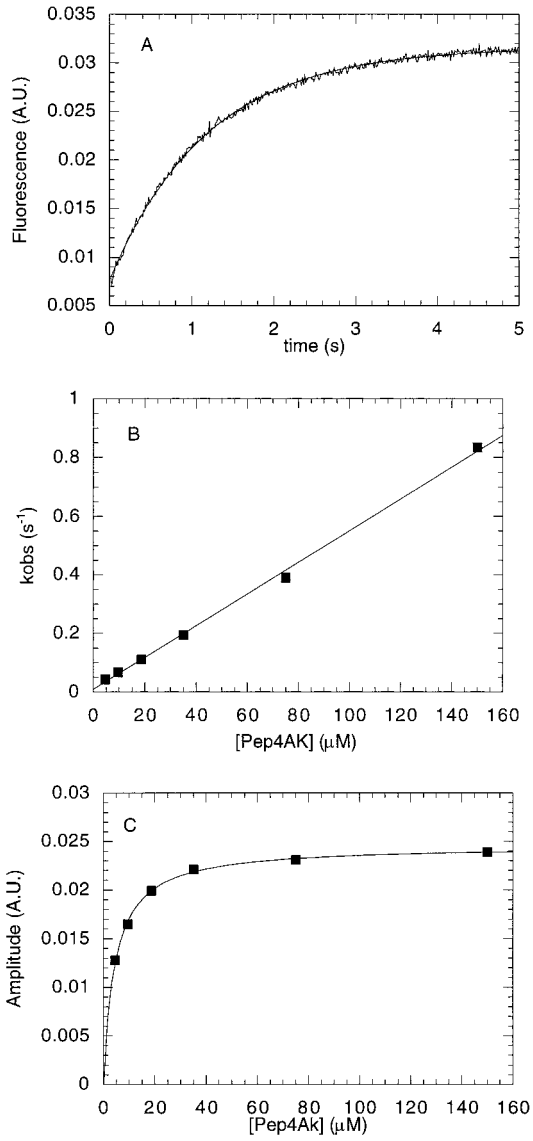

FIGURE 1: Protein fluorescence changes upon association of Pep4AK with the NS3 protease domain. Protein fluorescence at >305 nm was measured upon excitation at 280 nm on a stopped-flow instrument. To 100 nM NS3 protease in 50 mM Tris, pH 7.5, 15% glycerol, 1% CHAPS, and 1 mM DTT were added increasing amounts of Pep4AK dissolved in the same buffer. (A) Fluorescence changes upon the addition of 150 μM Pep4AK as a function of time. Data were fitted to a first-order rate equation to determine the value of k_{obs}. (B) Plot of k_{obs} versus Pep4AK concentration. Data were fitted to eq 3 to derive values for k_{on}. (C) Plot of fluorescence amplitudes as a function of added Pep4AK. The equilibrium dissociation constant of the NS3−Pep4AK complex was derived from a fit of the data to eq 2.

the sole determinant of the enhanced cofactor affinity of NS3−J. The parameters determined for the V36L + Q86P double mutant are very similar to the data obtained for the V36L single mutant with an additional slight decrease in the dissociation rate constants.

Next, the effects of glycerol on both equilibrium and pre-steady-state parameters of complex formation were investigated using the NS3−J enzyme. Complexation of the cofactor with the free enzyme was monitored using fluorescence spectroscopy. Table 2 shows that a 28-fold increase in equilibrium dissociation constants occurs by diminishing the glycerol concentration from 30% to 0%. This increase is attributable to a 76-fold increase in the dissociation rate

Table 2: Equilibrium and Pre-Steady-State Parameters of Complex Formation with Pep4AK of NS3 Proteases from HCV Strains J, Bk, and the Bk V36L and Bk Q86P + V36L Mutants[a]

enzyme	glycerol (%)	K_d (μM)	k_{on} (M^{-1} s^{-1})	k_{off} (s^{-1})
Bk	30	260	1420	0.37
Bk V36L	30	18	9750	0.17
Bk Q86P + V36L	30	11	8700	0.09
J	30	4	5400	0.02
J	15	30	9360	0.28
J	0	112	13620	1.52

[a] All of the values were determined by monitoring protein fluorescence changes upon complex formation of 100 nM NS3 protease with increasing amounts of Pep4AK in 50 mM Tris, pH 7.5, 1% CHAPS, 1 mM DTT, and different concentrations of glycerol. k_{on} values were determined from the pre-steady-state changes in fluorescence as described under Materials and Methods and shown in Figure 1A,B. K_d values were obtained from plots of the amplitude of the fluorescence change versus [Pep4AK] as shown in Figure 1C. k_{off} values were calculated assuming a simple equilibrium according to the relationship $k_{off} = K_d k_{on}$.

constant, counterbalanced by a 2.5-fold increase in the association rate. This latter effect is probably related to an augmented viscosity at higher glycerol concentrations that is expected to affect diffusion phenomena. The result is an increase in the half-life of the NS3−Pep4AK complex from 0.4 s (in the absence of glycerol) to 35 s (in the presence of 30% glycerol). Due to the experimental difficulties arising from the pronounced glycerol dependence of NS3−Bk, we decided to perform all subsequent experiments with the enzyme from the HCV J-strain.

Stabilization of the NS3−Pep4AK Complex by Substrate Peptides. The equilibrium dissociation constants reported in Table 1 have all been obtained by monitoring the Pep4AK-dependent increase in enzyme activity in the presence of 20 μM substrate. We noticed that in the absence of glycerol the apparent K_d value for the complex with the J-strain enzyme decreased when the same experiment was performed in the presence of higher substrate concentrations (see below). This suggests that in the absence of glycerol the free enzyme and the enzyme−substrate complex have different affinities for the cofactor peptide. We wanted to investigate this apparent stabilization of the NS3−Pep4AK complex by the substrate in more detail. First, we attempted to determine the K_d value of the complex fluorimetrically in the presence of added substrate. To this purpose, we switched to a truncated version of the substrate peptide used so far, having the sequence Ac-DEMEECASHL (substrate **S2**). This peptide was used since it is turned over with a 4-fold lower efficiency with respect to the longer substrate (*27*), thereby allowing one to record fluorescence data over a longer time period with acceptable levels of substrate depletion (less than 20% during the whole titration experiment). Furthermore, this substrate contains no fluorescent groups that would interfere with the measurements. In the absence of glycerol, the addition of 300 μM of **S2** decreased the fluorimetrically determined K_d value for the NS3−Pep4AK complex from 112 to 19 μM, whereas in the presence of 15% glycerol a more modest decrease from 30 to 12 μM was observed. These data suggest that both glycerol and substrate concur in stabilizing the enzyme−cofactor complex, whereby the stabilization effect produced by the substrate decreases with increasing glycerol concentration. This interplay between glycerol and substrate differs between the J and Bk enzymes. In fact, at glycerol concentrations above 15% no additional

Scheme 1

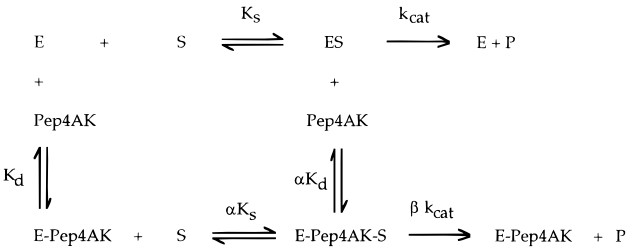

significant stabilization of the NS3−J−Pep4AK complex by the substrate can be observed. In contrast, for the Bk enzyme even in the presence of 30% glycerol a considerable discrepancy between the equilibrium dissociation constants obtained in the absence (260 μM, Table 2) and in the presence of 20 μM substrate **S1** (58 μM, Table 1) can be noticed.

We next wanted to analyze the influence of substrate binding on the stability of the NS3−Pep4AK complex in a quantitative way, taking into account the various equilibria involving enzyme, substrate, and cofactor that are described by Scheme 1, where E, S, and Pep4AK correspond to the enzyme, substrate, and Pep4AK activator, respectively. This scheme conforms to a model of nonessential activation, where substrate and activator bind to the enzyme in a random fashion (*28*). The constants describing the various equilibria are the following:

$$K_s = [E][S]/[E-S]$$

$$\alpha K_s = [E-Pep4AK][S]/[E-Pep4AK-S]$$

$$K_d = [E][Pep4AK]/[E-Pep4AK]$$

$$\alpha K_d = [ES][Pep4AK]/[E-Pep4AK-S]$$

The equation correlating the measurable steady-state velocity of substrate consumption with the equilibrium constants has been derived (*28*):

$$V = \frac{V_{max}S}{K_s\dfrac{(1+[Pep4AK]/K_d)}{(1+\beta[Pep4AK]/\alpha K_d)} + S\dfrac{(1+[Pep4AK]/\alpha K_d)}{(1+\beta[Pep4AK]/\alpha K_d)}} \quad (4)$$

In this equation, α is the factor by which K_d changes when all of the enzyme is present in the form of an enzyme−substrate complex. If all four enzyme species (E, E−S, E−Pep4AK, and E−Pep4AK−S) are at equilibrium, according to the mechanism in Scheme 1, the dissociation constant of S, K_s, must also change by the same factor α to αK_s once the enzyme is saturated with the activator. In other words, if the ternary enzyme−substrate−activator complex can be formed regardless of the path (through E and E−S or through E and E−Pep4AK), the thermodynamic stabilization of the ternary complex with respect to the two binary complexes will affect the affinity both for the substrate and for the activator by the same extent. Assuming that K_m is a good approximation of K_s for amide substrates of NS3, we would expect that the factor α by which a given substrate increases the affinity for Pep4AK should be quantitatively the same factor by which Pep4AK increases the affinity for the substrate. We attempted to verify this using both the substrate **S1** derived from the NS4A/NS4B cleavage site, described so far, and a substrate based on the sequence of

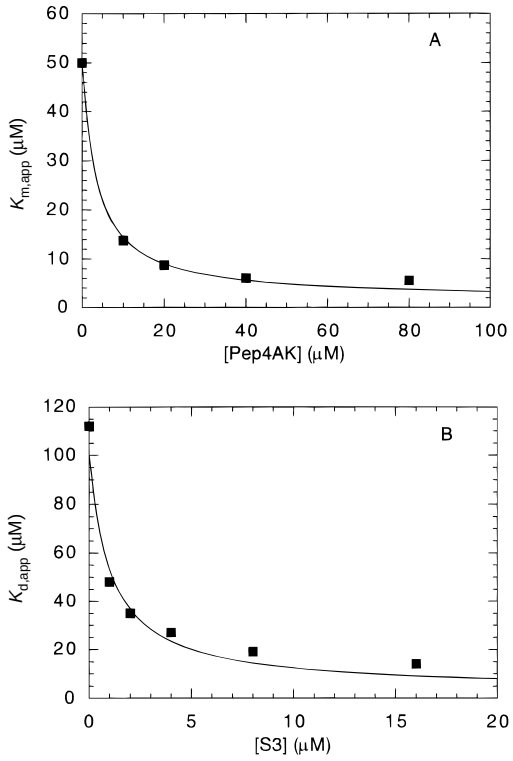

FIGURE 2: Increase of affinity for substrate and Pep4AK in the ternary enzyme−substrate−activator complex. The dependence of K_m values for substrate **S3** as a function of Pep4AK concentration (panel A) and the dependence of K_d values of the NS3−Pep4AK complex as a function of saturation by substrate **S3** (panel B) were determined kinetically using 10 nM NS3 protease in 50 mM Tris, pH 7.5, 1% CHAPS, and 1 mM DTT. K_m values were calculated from substrate titration curves at fixed Pep4AK concentrations and fit to the Michaelis−Menten equation, and K_d values were obtained from Pep4AK titrations at the indicated substrate concentrations and fit to eq 2. The K_d value in the absence of substrate was determined fluorimetrically. α values were obtained from a fit of the data to eq 5.

the NS5A/5B junction of the HCV polyprotein, having the sequence EAGDDIVPCSMSYWTGA (substrate **S3**). For both substrates, kinetic parameters were determined in the absence of glycerol and in the presence of increasing cofactor concentrations. Data from different experiments were simultaneously fit to eq 4, and α values were derived from this fit. Assuming the validity of the equilibria depicted in Scheme 1, one can show that the apparent K_m values, $K_{m,app}$, obtained at different activator concentrations are related to α according to eq 5 (*28*):

$$K_{m,app} = K_m \frac{(1 + [Pep4AK]/K_d)}{(1 + [Pep4AK]/\alpha K_d)} \quad (5)$$

An analogous equation will describe the relationship between the apparent K_d values obtained at different substrate concentrations and α. To verify this, we determined apparent K_d values for Pep4AK at increasing substrate saturation. Figure 2 shows the plots of $K_{m,app}$ versus [Pep4AK] and $K_{d,app}$ versus [S] obtained for substrate **S3** , whereas Table 3 reports the α values obtained for both substrates using the three different procedures. A good agreement of the α values obtained either from the global fitting procedure or from the effects of [S] on $K_{d,app}$ or of [Pep4AK] on $K_{m,app}$ was observed, indicating that the kinetic model depicted in Scheme 1 is compatible with the experimentally observed equilibria involving enzyme, activator, and substrate.

Table 3: Stabilization of the Ternary Enzyme−Activator−Substrate Complex in the Presence of Two Different Substrates[a]

	α value	
method	substrate **S1**	substrate **S3**
$K_{m,app}$ versus [Pep4AK]	0.10	0.032
$K_{d,app}$ versus [S]	0.05	0.030
multicurve fitting	0.12	0.034

[a] Experiments were performed in 50 mM Tris, pH 7.5, 1% CHAPS, and 1 mM DTT. The stabilization of the ternary enzyme−substrate−Pep4AK complexes with substrates **S1** (Ac-DEMEECASHLPYK−NH_2) and **S3** (EAGD DIVPCSMSYWTGA) with respect to the two binary complexes was expressed in terms of α, as defined in Scheme 1. α was determined by monitoring the decrease of apparent K_m as a function of [Pep4AK] (Figure 2A), by monitoring the decrease of apparent K_d as a function of [S] (Figure 2B), or by simultaneous fitting of eq 4 to a family of substrate titration curves recorded at different [Pep4AK] concentrations.

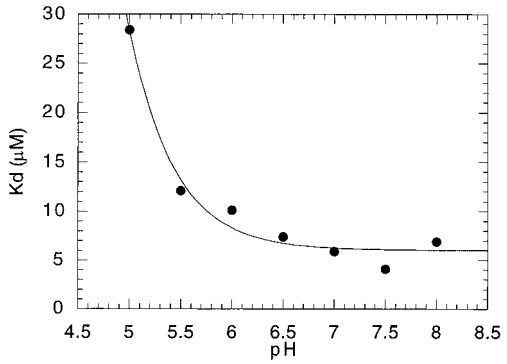

FIGURE 3: pH dependence of the equilibrium dissociation constant of the NS3−Pep4AK complex. NS3 protease (300 nM) in 25 mM Tris, 12.3 mM acetate, 12.3 mM Mes, 15% glycerol, 1% CHAPS, and 150 mM NaCl, adjusted to the indicated pH values, was titrated with increasing amounts of Pep4AK. Fluorescence spectra (λ_{ex} = 295 nm, emission 305−400 nm) were recorded upon each addition. The fluorescence intensity at 330 nm was determined from the spectra and plotted as a function of Pep4AK concentration. Equilibrium dissociation constants were obtained from this plot by a fit of the data to eq 2.

Influence of pH, Detergent, and Ionic Strength on Complex Formation. We next explored whether other physicochemical conditions may affect NS3−cofactor complex formation. Figure 3 shows the pH dependence of the equilibrium dissociation constant of the complex determined by fluorescence titration. We noticed that the stability of the NS3−Pep4AK complex was invariant over a pH range from 7 to 9 and decreased at lower pH. Subsequently, the effect of increasing ionic strength on the K_d value of the complex was determined in the absence of substrate and in the presence of 15% glycerol (Figure 4): an ∼10-fold decrease is observed by increasing the concentration of NaCl from 0 to 500 mM. Pre-steady-state analysis has shown that this effect was due to a decrease in the dissociation rate constant of the complex with little effect on k_{on} (Table 4).

We further explored the effect of different detergents on the K_d value of the NS3−Pep4AK complex. All data shown so far have been generated using 1% CHAPS as the detergent. Replacement of CHAPS by 0.05% Triton-X-100 or 0.05% LDAO resulted in a decrease from 3.7- (Triton, not shown) to 15-fold (LDAO, Table 4) in the K_d value of the complex. Addition of Triton or LDAO in the presence

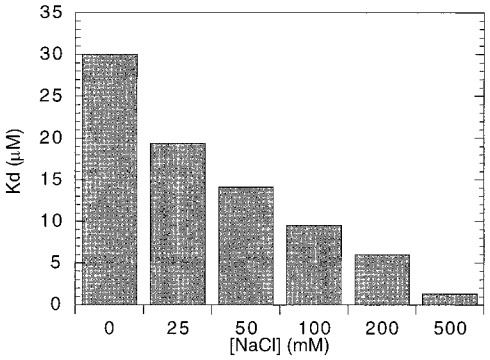

FIGURE 4: Ionic strength dependence of the K_d value of the NS3−Pep4AK complex. NS3 protease (300 nM) in 50 mM Tris, pH 7.5, 15% glycerol, 1% CHAPS, 1 mM DTT, and the indicated concentrations of NaCl was titrated with Pep4AK. Fluorescence spectra were recorded for each titration point, and equilibrium dissociation constants were calculated from fluorescence changes as described under Figure 3.

Table 4: NS3−Pep4AK Complex Stabilization by LDAO and NaCl[a]

detergent	[NaCl] (mM)	K_d (μM)	k_{on} (M^{-1} s^{-1})	k_{off} (s^{-1})	$t/2$ (s)
1% CHAPS	0	30	9360	0.28	2.4
1% CHAPS	500	1.3	21160	0.028	24
0.05% LDAO	0	1.9	4970	0.01	73
0.05% LDAO	500	0.2	8100	0.002	350

[a] All of the values were determined by monitoring protein fluorescence changes upon complex formation of 100 nM NS3 protease with increasing amounts of Pep4AK in 50 mM Tris, pH 7.5, 1 mM DTT, 15% glycerol, and the indicated amounts of detergent and NaCl. Rate constants were determined from the pre-steady-state changes in fluorescence as described under Materials and Methods. Complex half-lives were calculated according to $t/2 = \ln 2/k_{off}$.

of 500 mM NaCl resulted in a further decrease of the equilibrium dissociation constant. Under the best conditions, that is, 500 mM NaCl, 15% glycerol, and 0.05% LDAO, we determined $K_d = 200$ nM (Table 4). Again, pre-steady-state parameters indicate that this increased affinity is due to a marked decrease in the dissociation rate constant of the complex, leading to a half-life of 350 s. This value is almost 3 orders of magnitude higher than the half-life determined in the presence of 1% CHAPS and the absence of glycerol and salt.

Conformational Changes of the NS3 Protease as a Function of Physicochemical Conditions and Complex Formation with Pep4AK. We next wanted to investigate the influence of different physicochemical conditions on the solution structure of the J-strain NS3 protease domain complexed to its cofactor. To this purpose, limited proteolysis coupled to mass spectrometric detection of cleavage products was used as a technique. Limited proteolysis of NS3−J was performed using chymotrypsin, trypsin, Lys C, and subtilisin as proteolytic probes, and the experiments were monitored on a time-course basis under conditions of maximum NS3−Pep4AK complex affinity and under conditions of intermediate affinity (1% CHAPS, 15% glycerol). A detailed study on the influence of glycerol on the surface topology of NS3−BK will be published elsewhere (Orrú, S., Dal Piaz, F., Casbarra, A., Biasiol, G., De Francesco, R., Steinkühler, C. and Pucci, P. (submitted for publication).).

Fragments released from NS3−J under different experimental conditions were identified by mass spectrometry, leading to the assessment of cleavage sites. As an example, chymotrypsin rapidly cleaved NS3−J at Tyr6 releasing fragments 2−6 and 7−186. Subsequent cleavages were detected at Leu21, through identification of the peptides 7−21 and 22−186, and at Leu36 as shown by the occurrence of fragments 22−36 and 37−186 (not shown). Minor internal cleavage sites at Phe43, Trp53, Leu64, Tyr75, Tyr105, Tyr134, Phe154, and Cys159 were also observed at later stages of digestion. The overall results of the limited proteolysis experiments on the NS3 protease under different physicochemical conditions either in the absence or in the presence of saturating amounts of Pep4AK are reported in Table 5. The NS3 protease domain was digested in 1% CHAPS and 15% glycerol (K_d for cofactor peptide = 30 μM), showing a characteristic pattern: Tyr6 and Arg11 were the most accessible sites followed by Thr19, Leu21, and Arg24. All of these residues are located within the extreme N-terminal tail of the protease, thus indicating that in solution this segment is highly flexible and exposed. Protease-sensitive sites gathered into three separate regions of the protein, the N-terminal portion 36−75, the C-terminal segment 134−180, and the interdomain loop 92−109. When buffer composition was changed to high-affinity conditions, that is, 0.05% LDAO, 15% glycerol, and 500 mM NaCl (K_d = 0.2 μM) and chymotrypsin was used as conformational probe, the cleavage kinetics at the extreme N-terminal sites 6 and 21 were only marginally affected either in the absence or in the presence of Pep4AK (Figure 5A). However, under these conditions, the binding of the cofactor peptide led to a complete protection of Leu36, Phe43, Trp53, Leu64, and Tyr75, all located in the N-terminal domain, and of Tyr105 positioned within the interdomain loop (Table 5). These data suggest that, under high-affinity conditions, the association with the cofactor peptide had little effect on the extreme N-terminus where the segment containing the first 21 residues showed a high degree of conformational freedom. The N-terminal domain that is engaged in complex formation with Pep4AK was induced to adopt a more compact and tight conformation, displaying a dramatic decrease in proteolytic accessibility.

Conformational changes as a function of buffer composition could also be detected by fluorescence spectroscopy (Figure 5B). Changing buffer composition from 50 mM Tris, 1 mM DTT, 1% CHAPS, and 15% glycerol (spectrum 1) to 50 mM Tris, 1 mM DTT, 0.05% LDAO, 15% glycerol, and 500 mM NaCl resulted in a red shift of the emission maximum together with an increase in the fluorescence intensity (spectrum 3). In both cases addition of saturating amounts of Pep4AK went along with a blue shift of the emission maximum and an increase in intensity (spectra 2 and 4).

The Role of the N-Terminus of NS3 in Complex Stabilization. The results of our limited proteolysis experiments, indicating a high degree of mobility of the N-terminus of NS3 even after complexation with Pep4AK, were unpredicted since X-ray crystallographic data suggest an important role of the extreme N-terminus of NS3 in complex formation with the cofactor. In fact, in the crystal structure of the complex these residues contribute to the formation of strand A_0 and helix $\alpha 0$ that make extensive contacts with the cofactor and play a role in shielding Pep4AK from solvent. To investigate the role of this portion of the NS3 protease in the binding reaction with its cofactor peptide, we decided to produce a mutant protein (NS3−J−ΔN) in which the first 18 amino

Table 5: Limited Proteolysis Experiments Performed on NS3 Protease from the HCV J-Strain under Different Experimental Conditions Either in the Presence or in the Absence of the Cofactor Peptide Pep4AK[a]

protease	NS3 1% CHAPS	NS3−Pep4AK 1% CHAPS	NS3 0.05% LDAO/500 mM NaCl	NS3−Pep4AK 0.05% LDAO/500 mM NaCl
chymotrypsin	**Tyr6, Leu21, Leu36** Phe43, Trp53, Leu64, Tyr75, Tyr105, Tyr134, Phe154, Cys159	**Tyr6, Leu21** Leu64, Tyr75, Tyr134 Phe154, Cys159	**Tyr6, Leu21, Leu36** Phe43, Trp53, Leu64 Tyr75, Cys159, Met179	**Tyr6, Leu21** Tyr134, Phe154, Cys159 Met179
trypsin	**Arg11, Arg24** Lys62, Arg92, Arg109 Lys165, Arg180	**Arg11, Arg24** Lys62		
subtilisin	**Tyr6, Thr19, Leu36** Tyr75, Met74, Arg92 Arg109, Thr108, Tyr135	**Tyr6, Thr19**		
Lys C		**Lys26** Lys62, Lys165		

[a] All of the experiments were performed in the presence of 15% glycerol as described under Materials and Methods. Preferential cleavage sites are in bold.

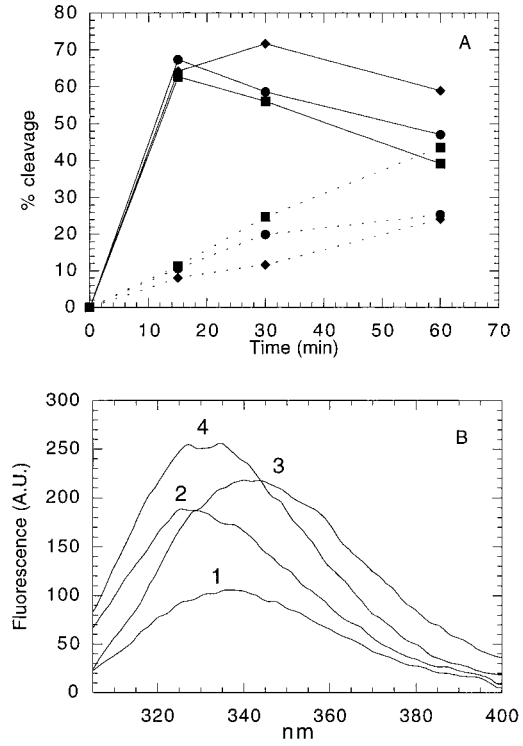

FIGURE 5: Conformational changes of the NS3 protease and its complex with Pep4AK under different physicochemical conditions. (A) The accessibility of NS3 to limited digestion by chymotrypsin was determined as described under Materials and Methods. The relative percentage of NS3 molecules cleaved after residue 6 (full lines) and after residue 21 (dotted lines) is shown as a function of incubation time. Experiments were performed under different conditions: 30 μM NS3 protease was incubated in 50 mM sodium phosphate, pH 7.5, 15% glycerol, and 1% CHAPS in the absence (dots) or in the presence (squares) of 80 μM Pep4AK. Alternatively, 30 μM NS3 protease was incubated in 50 mM sodium phosphate, pH 7.5, 500 mM NaCl, 0.05% LDAO, and 15% glycerol in the presence of 80 μM Pep4AK (diamonds). (B) Fluorescence spectra (λ_{ex} = 295 nm, emission 300−400 nm) of 250 nM NS3 protease in 50 mM Tris, pH 7.5, 15% glycerol, 1% CHAPS, and 1 mM DTT prior to (1) and after (2) the addition of 80 μM Pep4AK. Spectra were also recorded in 50 mM Tris, pH 7.5, 15% glycerol, 500 mM NaCl, 0.05% LDAO, and 1 mM DTT prior to (3) and after (4) the addition of 6 μM Pep4AK.

acids of NS3 have been deleted. This deletion is expected to eliminate A_0 and part of α_0 but to leave strand A_1 unaffected. The deletion was made in the context of a protease domain devoid of the solubilizing Lys tag at its C-terminus, and experiments were performed in parallel with an appropriate control enzyme. The deletion had only little effect on the catalytic properties of the enzyme as determined on substrate **S1**, resulting in a 30% decrease in k_{cat} and no alteration of K_m values (data not shown). To determine the effect of the deletion on the affinity of the enzyme for its cofactor peptide titration, we performed experiments under either "low-affinity" (no salt, 1% CHAPS) or "high-affinity" (500 mM NaCl, 2 mM LDAO) conditions monitoring protein fluorescence changes (Table 6). Under both conditions, the wild-type enzyme and NS3−J−ΔN had very similar equilibrium dissociation constants. These K_d values were, however, the result of dramatically different, but compensating effects on the individual association and dissociation rate constants (Table 6). Thus, under "high-affinity" conditions removal of the N-terminal 19 residues resulted in a 25-fold increase in on-rate, counterbalanced by a 90-fold diminished off-rate.

Table 6: Role of the N-Terminus of NS3 in Complex Formation with Pep4AK[a]

enzyme	detergent	[NaCl] (mM)	K_d (μM)	k_{on} (M^{-1} s^{-1})	k_{off} (s^{-1})
WT	1% CHAPS	0	10	18200	0.18
NS3−J−ΔN	1% CHAPS	0	15	120000	1.8
WT	0.05% LDAO	500	0.2	28700	0.005
NS3−J−ΔN	0.05% LDAO	500	0.6	710000	0.45

[a] All of the values were determined by monitoring protein fluorescence changes upon complex formation of 100 nM NS3 protease either wild type (WT) or with the deletion of the first 18 residues (NS3−J−ΔN) with increasing amounts of Pep4AK. At variance with all previous experiments, the proteases used in this experiment had no lysine tags at their C-termini. Experiments were performed in 50 mM Tris, pH 7.5, 1 mM DTT, 15% glycerol, and the indicated amounts of detergent and NaCl. Rate constants were determined from the pre-steady-state changes in fluorescence as described under Materials and Methods.

DISCUSSION

In the present work we attempted to address the different factors that influence the stability of the NS3−Pep4AK complex in solution. X-ray crystallography data show very tight interactions between the two molecules, with the cofactor peptide becoming an integral part of the fold of the N-terminal β-barrel of the NS3 protease domain. As already pointed out, Pep4AK is bound to a peculiar "molecular clamp" structure of the N-terminus of NS3, that adopts a

$\beta-\alpha-\beta$ fold with another β-strand contributed by Pep4AK intercalating into this fold. Such a complex is expected to be very tight, much tighter than the previously determined micromolar equilibrium dissociation constants (*25*). It is not clear to what extent crystal-packing forces contribute to the interaction. In this context, it is interesting to compare the two published crystal structures of the complex. Kim et al. (*13*) observe the $\beta-\alpha-\beta$ fold of the N-terminus of NS3 in only one molecule in the asymmetric crystallographic unit. In the other molecule the extreme N-terminus of the protease is not visible due to a high degree of conformational flexibility. The situation is different in the structure published by Yan and co-workers (*15*) where all molecules in the asymmetric unit adopt the same fold. In this case, however, a different crystal symmetry and consequently different crystal-packing interactions contribute to the stabilization of the fold (*15*).

In this work, we show that the affinity of the NS3 protease domain for its cofactor peptide is dramatically affected by physicochemical conditions, such as glycerol, salt, and detergent concentration, leading to differences in K_d values of almost 3 orders of magnitude. Furthermore, some of these effects were shown to be strain-specific with at least one determinant mapping to an NS3−NS4A interaction site. We reasoned that this dependence on physicochemical conditions may be related to the stabilization of the molecular clamp structure of the N-terminus of NS3. However, deletion of the first 18 amino acids of NS3 only slightly affected the equilibrium dissociation constant of the complex, although it did decrease the energy barrier for both the association and dissociation half-reactions, as monitored under pre-steady-state conditions. Together with results from limited proteolysis experiments, showing a high degree of accessibility of the N-terminal portion of NS3, which was only marginally affected by buffer composition or complex formation, the mutagenesis data indicate that the overall energetic contribution by the extreme N-terminus of the protease to Pep4AK−NS3 complex stability is relatively small. Possibly, the favorable contacts that the N-terminal A_0 strand makes with the cofactor are counterbalanced by the formation of the α-helical portion of the N-terminus (α_0) and the concomitant, energetically unfavorable solvent exposure of the hydrophobic residues Leu14, Ile17, Ile18, and Leu21 of NS3. This situation may lead, in solution, to very short half-lives of the "closed" conformation of the complex that is observed in the crystal structure, thus contributing little to the thermodynamic stability but still constituting a diffusion barrier affecting both the association and the dissociation rate constants of the complex. In vivo, the exposed, hydrophobic residues of helix α_0 may interact either with the N-terminus of the NS4A protein or with the membrane environment into which the complex has been shown to be anchored (*19*). This interaction may prevent their solvent exposure and thereby favor the formation of the molecular clamp structure at the N-terminus of the protease. Therefore, in the context of the full-length NS3−NS4A complex, the interactions with the extreme N-terminus of NS3 may become energetically important and may account for the tightness of the interaction between the two full-length binding partners. Data obtained on transiently expressed full-length NS3/NS4A complexes are in line with this assumption: thus, Bartenschlager and co-workers (*23*) reported that deletion of either 7 or 14 residues from the N-terminus of NS3 did not affect proteolytic activity but abolished detectable co-immunoprecipitation of the two binding partners, suggesting a severe impairment of complex stability. Despite these differences, it has to be pointed out that the stability of the complex between the two full-length binding partners has been shown to depend on similar physicochemical requirements as observed with the truncated NS3−Pep4AK complex (Gallinari, P. (manuscript in preparation).).

Tightening of the NS3−Pep4AK interaction under certain physicochemical conditions must therefore rely on driving forces other than the stabilization of a particular fold of the extreme N-terminus of NS3. A possible explanation comes from the recently solved NMR solution structure of the NS3 protease domain obtained in the absence of the cofactor (*29*). According to these structural data, the absence of NS4A results in a considerable conformational flexibility of the whole N-terminal β-barrel. Enhancement of the compactness of this part of the molecule is expected to result also in an increased stability of the enzyme−cofactor interaction that involves this region. Following this reasoning, one could explain the observed stabilization of the NS3−Pep4AK complex with increasing salt concentration by the strengthening of hydrophobic interactions at increased ionic strength that may result in an improved compactness of the N-terminal domain of the enzyme. Glycerol may have analogous effects. In fact, the enhancement of protein stability by glycerol has been proposed to arise by "preferential hydration" of the protein, that is, by exclusion of the cosolvent molecules from the surface−solvent interface (*30*, *31*). This exclusion is thermodynamically unfavorable, leading to a tendency of the system to decrease the protein−solvent contact area thereby promoting protein compactness. The effect of both glycerol and NaCl is to decrease the dissociation rate constant of the enzyme−cofactor complex with little effect on the on-rate. This is compatible with an antichaotropic effect of both buffer additives, contributing to a generic stabilization of the fold of the NS3−Pep4AK complex. Changes in the protein fluorescence spectrum as a function of buffer composition as well as limited enzymatic digestion experiments corroborate this hypothesis. In fact, glycerol and NaCl, as well as complex formation with Pep4AK itself, did not significantly affect the proteolytic pattern of the extreme N-terminus of NS3 but primarily affected the kinetics with which internal cleavage sites, especially those located in the N-terminal β-barrel, were recognized by added proteases such as chymotrypsin.

The stabilization of the NS3−Pep4AK complex by substrate peptides most likely relies on a mechanism similar to that of the stabilization by antichaotropic agents. As a matter of fact, substrate-induced complex stabilization was most evident at low glycerol concentrations and disappeared at higher concentrations of this buffer additive, suggesting that both substrate and glycerol concur in stabilizing the NS3−Pep4AK complex by the same mechanism. The threshold glycerol concentration above which no substrate-induced stabilization of the enzyme−cofactor complex was evident differed between J- and Bk-strain enzymes, being higher for the latter. Landro and co-workers (*32*) have analyzed the multiple interactions between the NS3 protease, its substrate, and the cofactor peptide. They concluded that prime-side residues of active site ligands bind to the enzyme in an NS4A-dependent fashion. This is in line with the notion that the prime-side binding pockets of the enzyme are located

on the N-terminal domain where the interaction with NS4A also occurs. Comparison of the X-ray crystal structures obtained in the presence or in the absence of cofactor has indeed shown significant differences in this region of the enzyme due to the formation, in the complex, of a new binding surface generated by the presence of the cofactor and a repositioning of enzyme loops (*24*).

Steady-state kinetic data, compatible with an ordered binding of NS4A and the substrate peptide, with NS4A binding first in the catalytic cycle have been published by Landro and co-workers (*32*). In contrast to that report our data are compatible with a random mechanism of activator and substrate binding according to Scheme 1. Since the NS3 protease is sparingly active also in the absence of its cofactor, complex formation with Pep4AK prior to substrate binding is not an absolute, mechanistic requirement for the cleavage of peptide substrates. An ordered mechanism, as proposed by Landro et al., will differ from Scheme 1 by the absence of an equilibrium between the binary enzyme−substrate complex and the ternary enzyme−substrate−activator complex. In other words, Pep4AK should not be able to bind once the enzyme−substrate complex is formed. However, we have found in stopped-flow experiments that increasing substrate concentrations did not affect the association rate constant of Pep4AK, whereas they did decrease its off-rate (not shown), indicating that the enzyme−substrate complex is still able to bind the cofactor. An intrinsically random mechanism of activator and substrate binding may nevertheless appear to be ordered in a steady-state analysis if under a given set of conditions (buffer composition, range of substrate, and activator concentrations) one particular pathway of ternary complex formation is strongly favored. Due to the dramatic influence of buffer composition on the affinity of the NS3−Pep4AK complex, the discrepancy between our study and the results published by Landro and co-workers may well be related to the different experimental conditions under which the experiments have been performed.

A random mechanism of substrate and activator binding predicts that the thermodynamic stabilization of the ternary enzyme−activator−substrate complex will affect the affinity for both activator and substrate to the same extent. This was verified for peptide substrates derived from both the NS4AB and NS5AB cleavage sites. The strengthening of enzyme−substrate interactions resulting from this mechanism thus contributes, together with the proposed NS4A-induced alignment of the catalytic triad (*13*−*15*, *24*), to the activation mechanism of the NS3 protease by its cofactor.

REFERENCES

1. Choo, Q.-L., Kuo, G., Weiner, A. J., Bradley, L. R. D. W., and Houghton, M. (1989) *Science 244*, 359−362.
2. Kuo, G., Choo, Q.-L., Alter, H. J., Gitnick, G. L., Redecker, A. G., Purcell, R. H., Myamura, T., Dienstag, J. L., Alter, M. J., Syevens, C. E., Tagtmeier, G. E., Bonino, F., Colombo, M., Lee, W.-S., Kuo, C., Berger, K., Shister, J. R., Overby, L. R., Bradley, D. W., and Houghton, M. (1989) *Science 244*, 362−364.
3. Houghton, M. (1996) Hepatitis C Viruses, in *Fields' Virology* (Fields, B. N., Knipe, D. M., and Howley, P. M., Eds.) 3rd ed., pp 1035−1058, Lippincott-Raven, Philadelphia, New York.
4. Lohmann, V., Koch, J. O., and Bartenschlager, R. (1996) *J. Hepatol. 24*, 11−19.
5. Kim, D. W., Gwack, Y., Han, J. H., and Choe, J. (1995) *Biochem. Biophys. Res. Commun. 215*, 160−166.
6. Bartenschlager, R., Ahlborn-Laake, L., Mous, J., and Jacobsen, H. (1994) *J. Virol. 68*, 5045−5055.
7. Failla, C., Tomei, L., and De Francesco, R. (1995) *J. Virol. 69*, 1769−1777.
8. Tanji, Y., Hijikata, M., Hirowatari, Y., and Shimotohno, K. (1994) *J. Virol. 68*, 8418−8422.
9. Han, D. S., Hahm, B., Rho, H. M., and Jang, S. K. (1995) *J. Gen. Virol. 76*, 985−993.
10. Kolykhalov, A. A., Feinstone, S. M., and Rice, C. M. (1994) *J. Virol. 68*, 7525−7533.
11. Preugschat, F., Averett, D. R., Clarke, B. E., and Porter, D. J. T. (1996) *J. Biol. Chem. 271*, 24449−24457.
12. Steinkühler, C., Tomei, L., and De Francesco, R. (1996) *J. Biol. Chem. 271*, 6367−6373.
13. Kim, J. L., Morgenstern, K. A., Lin, C., Fox, T., Dwyer, M. D., Landro, J. A., Chambers, S. P., Markland, W., Lepre, C. A., O'Malley, E. T., Harbeson, S. L., Rice, C. M., Murcko, M. A., Caron, P. R., and Thomson, J. A. (1996) *Cell 87*, 343−355.
14. Love, R. A., Parge, H. E., Wickersham, J. A., Hostomsky, Z., Habuka, N., Moomaw, E. W., Adachi, T., and Hostomska, Z. (1996) *Cell 87*, 331−342.
15. Yan, Y., Li, Y., Munshi, S., Sardana, V., Cole, J., Sardana, M., Steinkühler, C., Tomei, L., De Francesco, R., Kuo, L., and Chen, Z. (1998) *Protein Sci. 7*, 837−847.
16. Yao, N., Hesson, T., Cable, M., Hong, Z., Kwong, A. D., Le, H. V., and Weber, P. C. (1997) *Nat. Struct. Biol. 4*, 463−467.
17. Failla, C., Tomei, L., and De Francesco, R. (1994) *J. Virol. 68*, 3753−3760.
18. Lin, C., Thomson, J. A., and Rice, C. M. (1995) *J. Virol. 69*, 4373−4380.
19. Tanji, Y., Hijikata, M., Satoh, S., Kaneko, T., and Shimotohno, K. (1995) *J. Virol. 69*, 1575−1580.
20. Shimizu, Y., Yamaji, K., Masuho, Y., Yokota, T., Inoue, H., Sudo, K., Satoh, S., and Shimotohno, K. (1996) *J. Virol. 70*, 127−132.
21. Steinkühler, C., Urbani, A., Tomei, L., Biasiol, G., Sardana, M., Bianchi, E., Pessi, A., and De Francesco, R. (1996) *J. Virol. 70*, 6694−6700.
22. Tomei, L., Failla, C., Vitale, R. L., Bianchi, E., and De Francesco, R. (1995) *J. Gen. Virol. 77*, 1065−1070.
23. Bartenschlager, R., Lohmann, V., Wilkinson, T., and Koch, J. O. (1995) *J. Virol. 69*, 7519−7528.
24. Love, R. A., Parge, H., Wickersham, J. A., Hostomsky, Z., Habuka, N., Moomaw, E. W., Adachi, T., Margosiak, S., Dagostino, E., and Hostomska, Z. (1998) *Clin. Diagn. Virol. 10*, 151−156.
25. Bianchi, E., Urbani, A., Biasiol, G., Brunetti, M., Pessi, A., De Francesco, R., and Steinkühler, C. (1997) *Biochemistry 36*, 7890−7897.
26. De Francesco, R., Urbani, A., Nardi, M. C., Tomei, L., Steinkühler, C., and Tramontano, A. (1996) *Biochemistry 35*, 13282−13287.
27. Urbani, A., Bianchi, E., Narjes, F., Tramontano, A., De Francesco, R., Steinkühler, C., and Pessi, A. (1997) *J. Biol. Chem. 272*, 9204−9209.
28. Segel, I. H. *Enzyme Kinetics* (1993) John Wiley & Sons, Inc., New York.
29. Barbato, G., Cicero, D., Nardi, C., Steinkühler, C., Cortese, R., De Francesco, R., and Bazzo, R. (1999) *J. Mol. Biol.* (in press).
30. Timasheff, S. N. (1993) *Annu. Rev. Biophys. Biomol. Struct. 22*, 67−97.
31. Priev, A., Almagor, A., Yedgar, S., and Gavish, B. (1996) *Biochemistry 35*, 2061−2066.
32. Landro, J., Raybuck, S., Luong, Y. P. C., O'Malley, E. T., Harbeson, S. L., Morgenstern, K. A., Rao, G., and Livingston, D. J. (1997) *Biochemistry 36*, 9340−9348.

BI982773U